Article

Addressing Open Issues about the Structural Evolution of Methane Clathrate Hydrate

Demetrio Scelta, Samuele Fanetti, Selene Berni, Matteo Ceppatelli, and Roberto Bini*

Read Online

ACCESS | Metrics & More | Article Recommendations | Supporting Information

ABSTRACT: Methane is widespread in the Universe, and its occurrence is intimately connected with that of water, often as clathrate hydrate, likely the priority form in which methane is stored in icy moons, water-rich exoplanets but also in the depths of Earth's oceans. Arrangement and stability range of the crystalline structures, decomposition conditions, and miscibility of the resulting dense fluid mixtures are crucial for modeling the static and dynamic properties of these complex extraterrestrial environments and for identifying possible prebiotic reactive events under transient favorable conditions of pressure, temperature, and irradiation. Here, we report a high-pressure study of methane hydrate up to 4 GPa and 550 K. Ex situ synthesis of crystalline methane hydrate allowed the analysis of homogeneous samples by state of the art Raman and FTIR spectroscopy, accessing information which considerably expands and modifies our knowledge of the crystalline structures, of the decomposition conditions, and of the molten fluid's characteristics in a wide pressure and temperature range.
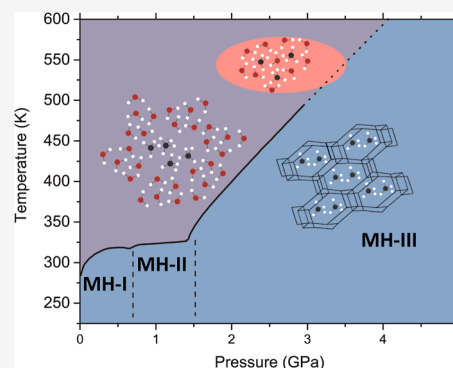
INTRODUCTION

Many reasons make methane clathrate hydrate the most studied among the hydrates of simple model molecules. The massive presence in the ocean depths and in the permafrost[1−4] represents at the same time not only an attractive energy resource but also a serious risk for the life on Earth.[5,6] In addition, water ices and hydrates are the most abundant "rocks" components in the outer solar system and a primary source of the volatiles trapped in icy bodies. Methane clathrate hydrate has a priority position, and it is thought to be one of the major methane species of the protoplanetary disk from which Saturn, the outer planets, and relative moons derive.[7−11] The persistence of methane at Titan's surface, where it is a major component of the atmosphere but a minor component of the surface,[11,12] can be explained assuming a methane supply source located at depth in the form of clathrate hydrate,[13] stable at Titan's deep interior pressure and temperature conditions,[14] and a dissociation driven by different processes like warming, sudden decompression, or chemical interactions with clathrate hydrate inhibitors. The pressure and temperature at which methane hydrate decomposes, as well as the effects that phase changes may have on the thermoelastic and transport properties, indicate that a precise knowledge of the phase behavior of methane hydrate by varying pressure and temperature is mandatory for modeling the static and dynamic properties of these icy planets and satellites.

The phase diagram of methane hydrate has been extensively studied in the last 20 years as a function of pressure by Raman, X-ray, and neutron diffraction experiments. An extensive overview of these studies is reported by Bezacier et al.[15] for

the P−T region relevant to Titan's interior.[16] There is a general consensus about the sequence of the different crystalline polymorphs upon compression at room temperature: at about 1 GPa, the cubic SI (MH-I) phase transforms into the hexagonal SH (MH-II), which at ∼2 GPa converts into the high-pressure *filled ice* structure FIS (MH-III). Around 40 GPa, a new hydrate phase (MH-IV) forms: methane molecules intercalate a water network isomorphic with hexagonal ice.[17] This phase is reported to be stable up to 150 GPa. On the contrary, there are only few inconsistent studies of the decomposition line above 1.5 GPa. The decomposition temperature at 3 GPa ranges from about 350 to 500 K,[15,18−20] with a suspicious perfect overlap with the ice VII melting in the study performed by Bezacier et al.[15] In all these studies, the samples are inhomogeneous with large excess of one component or with the presence of other species.[18]

Another intriguing aspect concerning the phase diagram of methane hydrate is the recent observation of a remarkably increased solubility of methane in water once the hydrate is decomposed at pressures exceeding 1 GPa.[21] The amount of methane dissolved in water is claimed to increase of more than 4 order of magnitude from the values measured at 0.2 GPa,
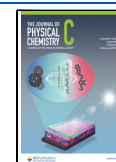
10^{-3} to 10^{-2} mole percent (mol %) depending on temperature,[22] reaching a sort of saturation around 44 mol % at 1.9 GPa and 373 K. A combined neutron scattering experiment and ab initio molecular dynamics simulation analyzed the structure of the mixed fluid around 2 GPa, evidencing the conservation of the hydrogen-bonded network and an enhanced interaction among methane and water molecules likely driven by a slight increase in the methane dipole moment.[23] Such increased miscibility with compression is not only relevant for a better understanding of the hydrophobic interactions[24] but also because elementary chemical processes induced photochemically, thermally, or by static or impulsive pressures can be remarkably enhanced. In fact, the high-pressure photoinduced reactivity of clathrate hydrates has been shown to be rather scarce, being dictated, and limited by the constraints due to the confinement in the rigid polyhedral hydrogen bonded water network.[25−27] Such constrains are removed in the fluid phase, and in combination with the high density attainable at high pressure, the reactivity can be greatly enhanced.[28] This issue is of interest as a potential channel, exploiting transient molten ices originated by cryovolcanism or impact phenomena with astronomical objects, for the prebiotic synthesis of several simple organic molecules detected on planet and satellite surfaces.[29]

For all these reasons, we investigated the lattice phonon spectrum of methane hydrate through the MH-I, MH-II, and MH-III phases, its decomposition from the three phases, and the behavior of the melt as a function of pressure and temperature by exploiting homogeneous crystalline samples synthesized ex situ and filling the entire sample chamber. Infrared absorption spectroscopy was employed for the characterization of the clathrate decomposition, whereas an accurate study of the lattice phonons and of the melt composition was performed as a function of pressure and temperature using Raman spectroscopy with high spatial resolution. The characterizing features of the lattice phonon region, an important indirect structural information, and the melting conditions of all the three phases were identified. In addition, the miscibility of the fluid was investigated in a large portion of the P−T space finding considerably different results with respect to the existing literature.

■ METHODS

Crystalline methane hydrate was prepared ex situ by means of a specifically designed high-pressure stainless-steel vessel. This was filled with finely ground ice and cooled to 160 K using a bath of coexisting solid and liquid ethanol. The vessel was sealed by means of silver-plated gaskets and then pumped for hours before loading methane while maintaining the vessel at 160 K. The methane (purity >99.99%) pressure was raised up to 200 bar at this temperature. After about 30 min, the vessel is transferred to an ethyl glycol bath cooled at 243 K using a chiller. The temperature was then increased according to the following steps: from 243 to 271 K in 1 h; from 271 to 280 K in 4 h, and in other 4 h from 280 K to ambient. The gas pressure increased up to 350−400 bar (271 K) to decrease to 40 bar after the cycle completion. Once the cycle was completed, the vessel was placed in liquid nitrogen where it was unsealed. The crystalline product, considerably unstable at ambient temperature, was rapidly transferred in the membrane anvil cell employed for the high-pressure measurements by placing a few crystals on top of the anvils together with some ruby chips employed for determination of the pressure by the

ruby fluorescence method.[30] During this operation, the cell was kept cold using liquid nitrogen which also ensured a dry atmosphere to minimize CO_2 contamination. Once the sample was loaded, the cell was closed, and the membrane pressurized. The cell was equipped both with sapphires, culets ranging between 600 and 950 μm, and Cu−Be gasket drilled to a diameter of 450 μm, for characterizing the melting conditions by FTIR spectroscopy, and diamonds IIas, 400 μm culets, and stainless-steel gaskets drilled to a diameter of 150 μm, employed in all the Raman experiments. High temperature was achieved by resistive heating measuring the temperature with a K-type thermocouple placed close to the anvils with a 0.1 K accuracy. IR absorption spectra were measured using a Bruker IFS-120 HR Fourier transform IR spectrometer equipped with a globar lamp, KBr beam splitter, and MCT detector. An optical beam condenser made by ellipsoidal mirrors was used to focus the IR beam to a spot size comparable to the dimensions of the sample contained in the sapphire anvil cell.[31] Raman measurements were performed using the 660 nm line of a diode laser as an excitation source. A backscattering geometry was adopted for the experiment using a long working distance 20× Mitutoyo micro-objective. The spatial resolution on the sample was about 3 μm.[32] Spectra were collected using an Acton/SpectraPro 2500i monochromator equipped with holographic super notch filters and a CCD detector (Princeton Instruments Spec-10:100BR). The resolution used in both FTIR and Raman experiments is 1 cm^{-1}.

■ RESULTS AND DISCUSSION

Methane clathrate hydrate was prepared as MH-I ex situ and loaded in a diamond (DAC) or sapphire (SAC) anvil cell, as
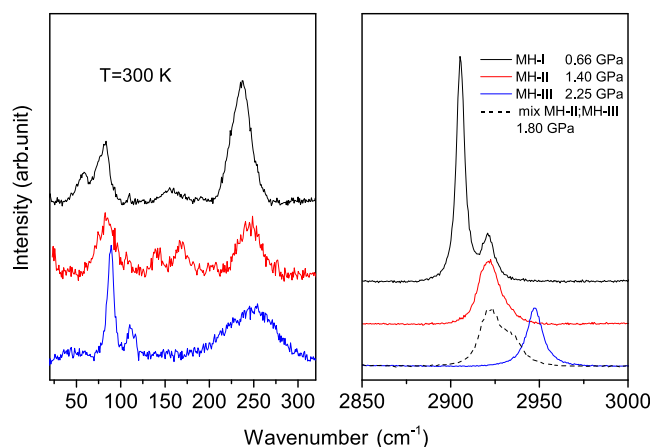

Figure 1. Representative room-temperature Raman spectra acquired on compression in the three crystal phases of methane clathrate hydrate both in the lattice phonons region (left) and in the C−H stretching region (right). The dashed spectrum in the right panel has been acquired at the MH-II to MH-III transition, showing the coexistence of the two phases.

described in the Methods section. The samples were compressed at room temperature monitoring the evolution of the Raman spectrum. While the C−H stretching region is well characterized in phases MH-I and MH-II,[33,34] only few data are reported for the lattice phonon region and limitedly to the MH-I phase.[35,36] The MH-II to MH-III transition is often characterized by demixing of the components with formation
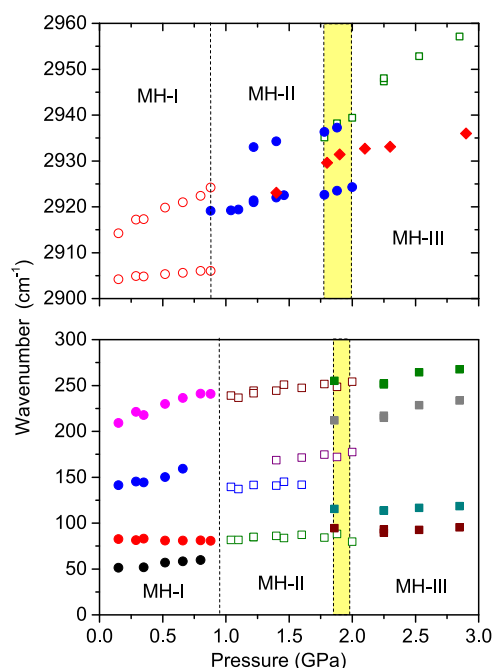
Figure 2. Pressure shift of lattice phonons (lower panel) and C−H stretching modes (upper panel) across the three methane hydrate phases. In the upper panel, the red diamonds are the frequencies of the mode measured in pure methane.[15] The dashed lines indicate the pressures of the phase transitions. The small differences between their values in the two panels are related to the different spectral responses in the two regions. Yellow areas indicate the region where coexistence of MH-II and MH-III phases is observed.

of ice VI and methane in phase I. This occurrence, observed in some of our experiments and already reported by others,[15,33,34] led also to an erroneous assignment of the C−H stretching peak of crystalline methane to MH-III.[33,34] The C−H stretching band of MH-III is easily recognized because its frequency is about 10 cm^{-1} higher than that of the MH-II peak.[15,37−39] Exploiting the ex situ preparation of the hydrate, we succeeded to have homogeneous samples inside the cell (see Figure S1), which is a prerequisite to have a reliable sample to follow the structural evolution. High-quality MH-III samples were produced by slowly crossing the MH-II−MH-III transition. The two phases coexist at the microscopic level (2− 3 μm is the spatial resolution) at room temperature between 1.75 and 2.0 GPa, as shown in Figure 1. In the same figure, we also report the characteristic lattice phonon spectra of the three phases.

The lattice phonons spectra, reported here for the first time for phases MH-II and MH-III, present very distinctive features in the three phases. Four phonon bands are detected with certainty in all the phases, and their pressure evolution is reported in Figure 2. Other very weak peaks have been detected in some sample regions but because of their scarce reproducibility over the sample, we are not reporting their frequencies. Interestingly, the phonon spectra of the three hydrate phases resemble those characterizing two ice phases, III and V, existing only in a very restricted P−T range (0.2− 0.65 GPa and 218−273 K). In particular, the phonon spectra of MH-I and especially of MH-II resemble the one characterizing ice V, whereas the phonon spectrum of MH-III is just like that of ice III.[40] It is worth commenting that despite the MH-III structure is reported to possess an
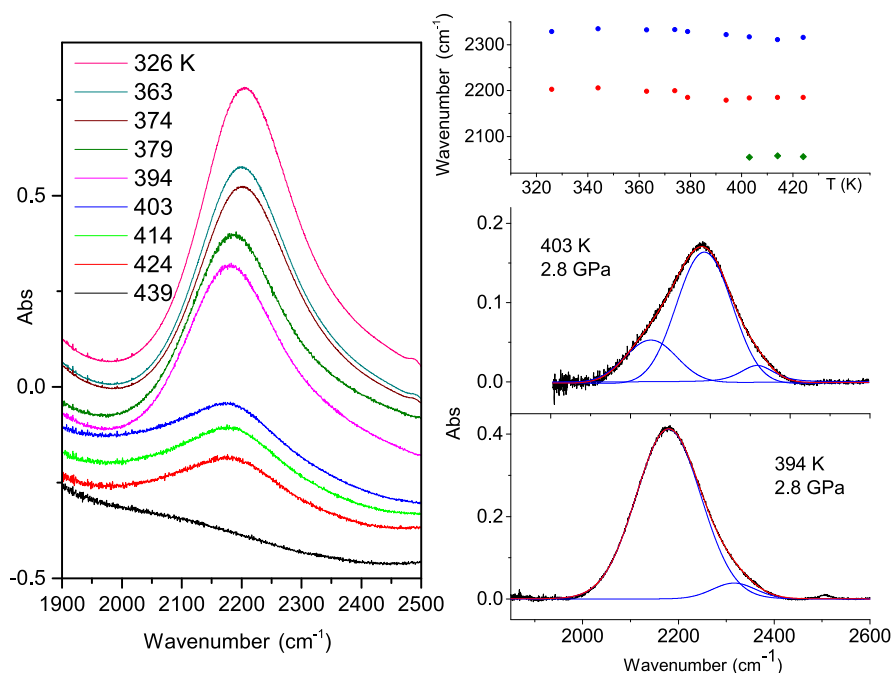

Figure 3. Temperature evolution of the IR absorption of a combination band of water, bending plus H-bond libration ($\nu_2 + L$), in crystalline hydrate MH-III up to its decomposition. On the left, the IR absorption spectra, vertically translated for the sake of clarity, showing the two abrupt intensity changes at 403 and 435 K, which have been ascribed to the melting of ice VII (403 K) finely dispersed across the sample, and to the methane hydrate decomposition (435 K). On the right, the deconvolution of this band after baseline correction and using Gaussian peaks is shown. The spectrum measured at 394 K is typical of the crystal phase (see S4). The spectrum measured at 403 K has been acquired immediately after the observation in vivo of an abrupt change in the interferogram. In the upper right panel, the temperature evolution of the peak frequency of the three bands is also reported.
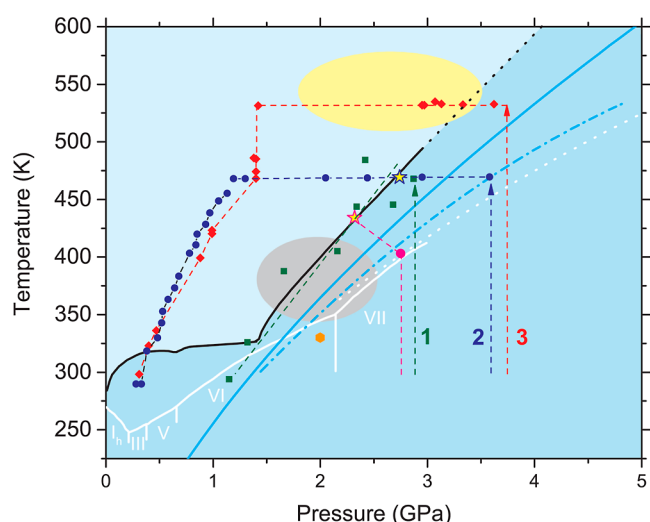
Figure 4. Experimental paths followed to study the miscibility of water and methane in the fluid phase. The three paths followed are indicated by different colors: path 1 green arrow and solid squares; path 2 blue arrow and solid circles; and path 3 red arrow and solid diamonds. We also report the path (magenta) followed to study the decomposition of MH-III with the full circle, indicating the ice VII melting and the magenta/yellow star the decomposition of MH-III. The blue/yellow star indicates the appearance of a biphasic fluid during the isothermal decompression at 469 K. The black line indicates the decomposition of methane hydrate by Dyadin et al.[46] up to 1.5 GPa and by Kurnosov et al.[18] for higher pressures. The melting lines of CH_4 are reported as full[50,51] and dash-dot[52] cyan lines; the full white lines refer to the phase diagram of water from ref 53, whereas the dashed white line shows the melting of water ice from ref 54. The decomposition line by Bezacier et al.[15] is not reported. which is coincident with a study by Dyadin et al.[46] up to 1.5 GPa and following the melting line of ice VI and VII for higher pressures. The gray region indicates the P−T conditions where an increased miscibility is reported in refs 21 and 23, while the orange full hexagon is where a homogeneous appearance of the fluid with 19 mol % of methane is reported in ref 21. The light yellow region is where we have observed a rather homogeneous distribution of methane within the fluid.

arrangement of the water molecules analogous to that of ice Ih,[41] the phonon spectrum is completely different presenting sharp and strong features around 100 cm^{-1}, whereas the lattice phonon spectrum of ice Ih presents at ambient pressure Raman intensity only above 200 cm^{-1}.[40,42]

As far as the pressure shifts are concerned, we observe a perfect agreement with the lattice phonon data of phase MH-I reported by Sasaki et al.,[35] including the negative pressure shift of the higher component of the low-frequency doublet. In phase MH-II, the pressure shifts of all the phonon bands undergo to a significant decrease in the slopes (see Table S1), which are substantially preserved in phase MH-III.

FTIR spectroscopy was employed to detect the clathrate hydrate decomposition. This method, already used to monitor the decomposition and crystallization dynamics of Ar hydrate,[43] relies on a huge red shift and intensity decrease in a combination band of water, bending plus H-bond libration ($\nu_2 + L$), during the melting. This band is located between 2000 and 2250 cm^{-1}, therefore not accessible using the DAC, due to the strong IR absorption of the diamond phonon, but detectable once sapphires are employed as anvils. The evolution of this band during the decomposition of MH-I and MH-II is shown in Figures S2 and S3. The decomposition is accompanied by a frequency drop larger than 130 cm^{-1}, not

appreciably changing with pressure (0.6, 0.7, and 0.9 GPa). This shift exceeds that observed in Ar hydrate at 0.66 GPa (∼100 cm^{-1})[43] and in pure ice at ambient pressure[44] (∼70 cm^{-1}). This difference has to be entirely ascribed to the frequency of the water band in the fluid which red shifts from about 2150 cm^{-1} in pure water to 2090 cm^{-1} in the fluid obtained by the methane hydrate decomposition. A red shift of this combination band has been reported in the presence of chaotropic ions,[45] thus suggesting a reduction of the H-bond network strength due to the presence of methane. The decomposition temperatures measured in MH-I (0.6 and 0.7 GPa) and in MH-II (0.9 GPa) are in nice agreement with the ones reported by Dyadin et al.[46] As already reported for the phase HS-III of Ar hydrate,[43] the direct recrystallization from the melt is achieved here in all the three cases once the samples are supercooled by 3−6° (right panel in Figure S3). The time evolution of the forming crystal spectrum nicely agrees with the kinetics measured in Ar hydrate (see Figures S4 and S5) considering the time window where the long-range crystalline order is built.[43]

Contrary to the general consensus about the P−T decomposition conditions of MH-I and MH-II, the literature data concerning the decomposition of MH-III are anything but consistent.[15,18−20] A decomposition line perfectly overlapping with the ice VII melting was depicted using Raman spectroscopy by Bezacier et al. up to 5 GPa.[15] Using the same technique, a decomposition line located at considerably higher temperatures (about 75 K at 2.8 GPa) was found by Kurnosov et al.,[18] but the presence of ammonia in the sample raises an issue about the reliability of these data. Recent Raman[19] and synchrotron X-ray diffraction[20] studies analyzed the decomposition of MH-III up to 40 GPa. Above 2.5 GPa, the dissociation line lies below the melting lines of both ice VII and methane. Decomposition of MH-III into these phases should give rise to a volume increase of ∼20% (volume data from refs 41, 47, and 48), which is difficult to reconcile with the almost flat evolution with pressure of the decomposition line. These discrepancies are likely not only due to the nature of the samples, that is, the actual presence of the hydrate phase MH-III and the amount of water ice, two issues related to the already discussed difficulties in obtaining pure MH-III crystals, but also to the intrinsic water release going from MH-I to MH-II and then to MH-III. The procedure we employed for studying the decomposition in phases MH-I and MH-II turned out to be rather challenging when applied to phase MH-III because of the recurring sapphires rupture on increasing temperature above 2 GPa. We succeeded to complete an experiment where the decomposition process was accurately followed, as reported in Figure 3.

A MH-III sample homogeneously distributed within the volume cell was brought to 2.8 GPa and then isobarically heated while monitoring the IR spectrum. At 403 K, an abrupt intensity decrease (about 50%) of the crystal absorption band was observed. Deconvolution of the experimental spectra (see Figure 3) shows that to the typical spectrum of the solid hydrate, with a strong peak centered at about 2200 cm^{-1} and a much weaker one at higher frequency, adds a low frequency peak due to the formation of liquid water.[44] These conditions coincide with ice VII melting, but, since the central peak (MH-III crystal band) persists also at higher temperatures, the melting is only partial and ascribable to excess ice VII only. On further heating, the pressure progressively dropped, but the spectrum did not further changed up to 434 K (2.3 GPa),
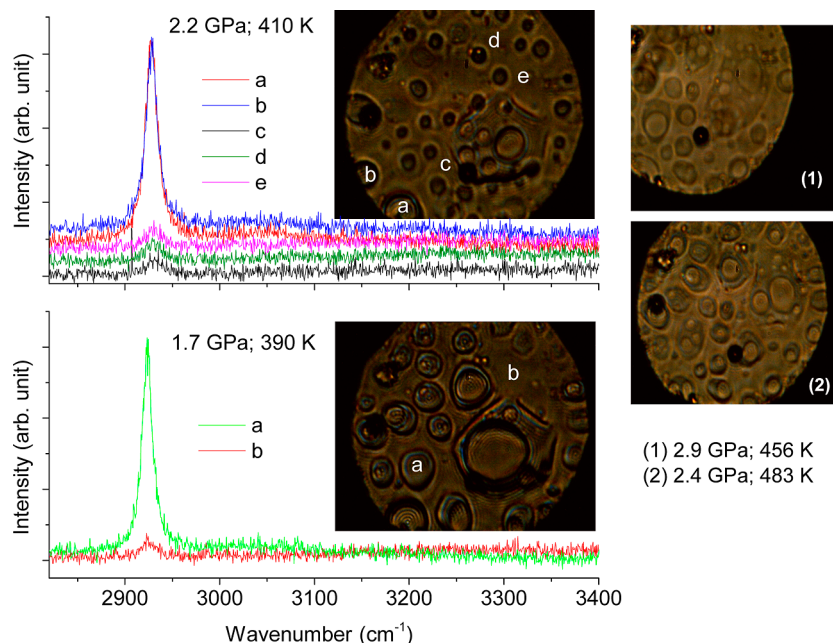
Figure 5. Right: sample pictures acquired after the melting of MH-III while releasing the pressure above 450 K (path 1 in Figure 4). Left: Raman spectra acquired at the P−T conditions where in ref 21 an enhanced miscibility is reported (gray region in Figure 4). The sample points where the spectra have been measured are indicated by letters. The darker round regions are methane bubbles, whereas the homogeneous regions filling the space among the bubbles are water rich.
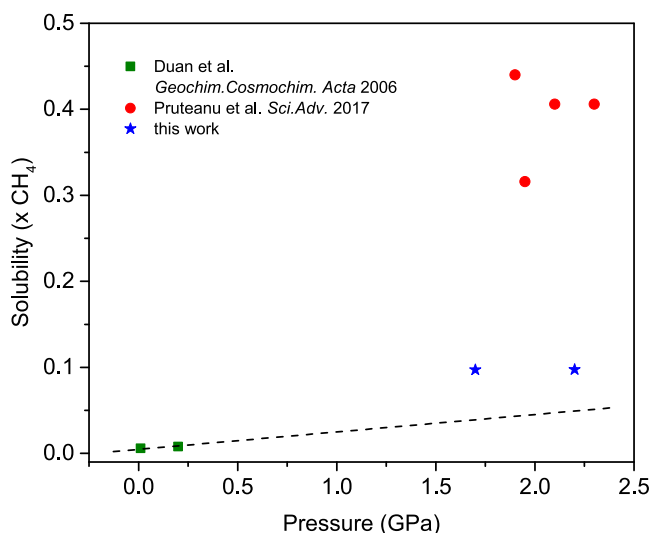

Figure 6. Comparison of methane solubility in water as a function of pressure. Values reported as green squares are relative to data computed at 363 K using a thermodynamic model based on a large set of experimental low-pressure values.[22] The dashed line is a linear extrapolation of this set of data. The red dots are few representative values from ref 21 obtained on fluid mixtures with an amount of methane ≤39%. The solubility has been determined from the relative extensions of water and methane-rich regions, as determined by sample micrographs. Blue stars data are from this work and have been obtained by the intensity ratio of the C−H stretching mode of methane measured inside the methane bubbles and in the water-rich regions of the sample.

where the absorption band of MH-III crystal suddenly disappeared. This temperature value, well above the melting line of pure methane, nicely agrees with the decomposition line proposed by Kurnosov et al.[18] Also in that case, the crystalline

hydrate homogeneously filled most of the sample region, thus permitting a reliable detection of the decomposition.

Finally, the last issue tackled in this study concerns the increased solubility of methane in water with rising pressure and temperature in the fluid phase. A thermodynamic model has been developed on the existing data for computing the methane solubility in water up to 573 K and 0.2 GPa.[22] Taking 363 K as a reference temperature, the solubility is reported to increase of 1 order of magnitude, passing from few tens of bars to 0.2 GPa and reaching a saturation (data fit by Boltzmann's sigmoidal equation) for molar fractions values of 7 to 8×10^{-3}. Recently, these findings were challenged by a high-pressure study, in which fluid samples containing 19 mol % of methane in water appeared visually homogeneous at 330 K and 2 GPa.[21] This was taken as an evidence that the saturated concentration in these P−T conditions exceeds 19 mol %. Raman spectra acquired in different sample regions confirmed a homogeneous distribution of methane across the sample. However, these pressure and temperature conditions are well inside the stability range of crystalline hydrate, ice VI, and solid methane, as reported in Figure 4, being therefore likely due to crystallized material. The amount of methane in the water-rich portions of the fluid was later determined in a sample richer in methane (58 mol %) by measuring the extension of the water-rich regions through micrographs and using the literature densities.[21] The molar fraction of methane dissolved in water was estimated to increase dramatically with pressure, reaching the maximum value, ~0.45, at about 2 GPa and 373 K and not increasing further up to 3.2 GPa. Ab initio molecular dynamics simulations confirmed the tendency, already reported,[49] to a reduction of the hydrophobic effect with increasing pressure but especially indicated the development of a small dipole moment (0.3 D) for methane above 1.2 GPa.[23]

To test the effective formation of a homogeneous fluid, a potentially attracting condition for inducing photochemical reactions, we compressed different samples of crystalline
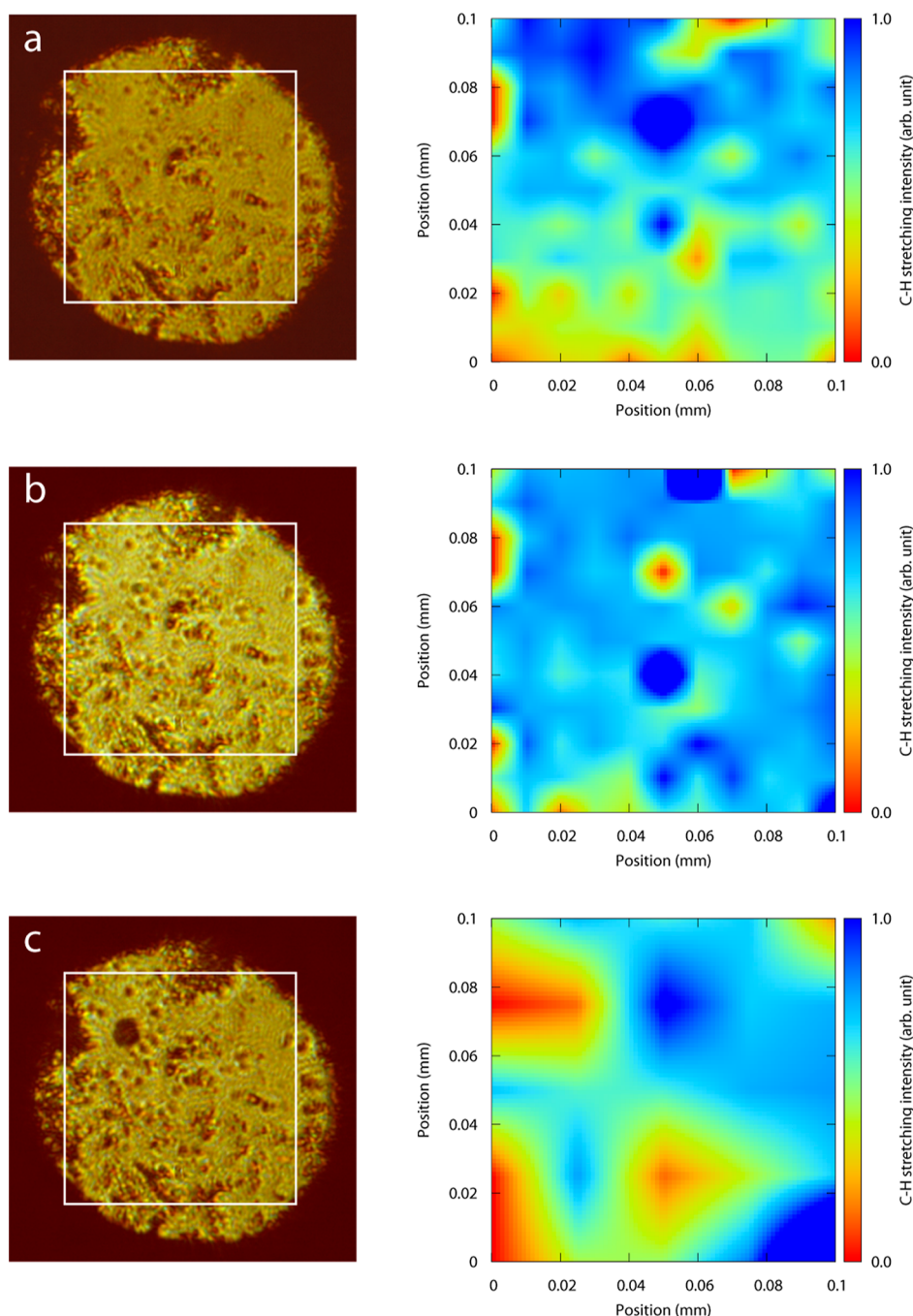
Figure 7. Raman maps (right) obtained by mesh acquisition of the C−H stretching region in steps of 10 μm in the regions evidenced by the white frame in the sample images reported on the left side. The color scale has been obtained by normalizing the intensity of the C−H stretching band of methane to the strongest one measured across the sample (dark blue) so that the reddish areas are those where methane is not detected. (a) 3.1 GPa and 536 K; (b) 3.0 GPa and 532 K after 72 h; and (c) 1.42 GPa and 531.5 K.

methane hydrate whose homogeneity and methane content, ≤14.8%, were verified by Raman spectroscopy (see Figure S1). The hydrate samples were compressed up to pressures ranging between 2.7 and 3.8 GPa and then isobarically heated, as shown in Figure 4. The sample heated up to 475 K at 2.7 GPa (path 1) always appeared, once molten, fully demixed (Figure 5). The sample was then brought back to ambient temperature and 1 GPa (phase MH-I) without observing any change in the aspect as well as in the Raman spectra: the strong C−H stretching band of methane was observed in the measurements performed within the bubbles, whereas it was barely visible in

the regions among the bubbles (Figure 5) and also at the P−T conditions where Pruteanu et al.[21,23] reported enhanced miscibility (gray region in Figure 4).

An estimation of the amount of methane in water-rich regions is attainable by the intensity ratio of the methane band in the two regions. The spectra have been acquired in the same conditions just moving the sample in the focal plane from one point to the other. The intensity ratio is almost identical in the two P−T points investigated: 10.31 at 1.7 GPa—390 K and 10.25 at 2.2 GPa—410 K. These ratios correspond to solubilities of 0.0970 and 0.0975 mol %, therefore much

lower than the values estimated from micrographs by Pruteanu et al.,[21] which are above 0.4 mol % in this P−T region, but closer to the values computed through a thermodynamic model constructed on the available low-pressure data[22] (see Figure 6). We also remark that our values represent an upper limit because we are probing a sample thickness of about 18 μm (given by the convolution of the waist length with the detection depth of field), therefore possibly probing also underlying water-rich regions when we measure methane bubbles or, conversely, methane bubbles when we measure water-rich regions, leading to an overestimation of the methane solubility in water.

In the second experiment, we extended the pressure range where the fluid was monitored at high temperature (470 K) releasing isothermally the pressure down to 1 GPa. The sample appearance is homogeneous at 3.5 and 3.0 GPa, but as the pressure drops to 2.7 GPa, the fluid appears completely demixed. These P−T conditions (blue star in Figure 4) nicely fit the decomposition line of MH-III suggested by Kurnosov et al.[18] and confirmed at lower P−T conditions in this work. Therefore, we ascribe the homogeneous appearance of the sample above 2.7 GPa to crystalline MH-III. Once the sample decomposes, it remains always biphasic during the entire cooling/decompression path until the recrystallization of phase MH-I occurs. In the third experiment, we heated the sample up to 535 K above 3.5 GPa. We slowly released pressure isothermally while performing Raman grid map acquisition (mesh) on the sample. At 3.3 GPa and 532.4 K, changes in the visual appearance of the sample may be suggestive of the melting occurrence, again in good agreement with the decomposition line by Kurnosov et al.[18] The mesh measured at close pressure and temperature conditions (steps of 10 μm) shows certain homogeneity in the methane distribution across the sample even though a leopard spot distribution remarks the presence of water and methane-rich regions [see panel (a) in Figure 7]. A Raman mesh acquired at the same pressure and temperature conditions after 72 h shows an increased homogeneity in the methane distribution all across the sample [see panel (b) in Figure 7], an observation suggestive of a possible kinetics of methane solubilization in water. The pressure was then lowered to 1.4 GPa where a new mesh was acquired. The formation of large water or methane-rich domains is rather evident anticipating the clear demixing visually observed once the temperature was isobarically lowered to 470 K.

CONCLUDING REMARKS

In summary, we have exploited the synthesis and the successful transfer in the DAC or SAC of homogeneous methane hydrate crystalline samples filling all the sample volume for addressing fundamental questions related to the phase behavior, the high-pressure—high-temperature melting conditions, and the solubility of hot compressed mixed methane—water fluids. Methane hydrate is one of the major methane species in the Universe likely representing a primary methane source in the outer Solar System, and the three issues tackled in this work are central for modeling static and dynamic properties of these icy bodies. The pressure and temperature region investigated is indeed relevant to Titan's interior, the second largest moon and the only planetary body in the Solar System having a hydrologic cycle like Earth but based on methane. Using Raman spectroscopy, we have characterized the lattice phonon region of the MH-II and MH-III phases, providing an important benchmark for testing the structural properties. The resemblance of the phonon spectrum of the phase MH-III to that of ice III instead of that of ice Ih, the matrix suggested to be filled by methane molecules, raises important questions about the appropriateness of the structure assignment or conversely about the entity of the lattice distortion due to the methane filling. Raman spectroscopy has also been used to carefully monitor the solubility of methane in the fluid, a very important issue to explain the prebiotic synthesis of organic material from molten ices exploiting irradiation or impact phenomena. We have found a solubility in line with that found at much lower pressure (few kilobars) and significantly lower than that recently reported, a discrepancy likely related to the estimation of the methane amount in the sample. Finally, FTIR spectroscopy was employed to characterize the decomposition of homogeneous samples filling the entire sample volume in all the three low-pressure phases, confirming the existing literature about phases MH-I and MH-II, and solving the contrasting results so far obtained for phase MH-III. Here, we evidence an unavoidable two-step mechanism where first occurs the melting of ice VII, present in the sample because of the progressive enrichment in methane of the hydrate going from phase I to III, and then, tens of degrees above, the decomposition of the hydrate takes place, thus moving the stability field of the hydrate well above that of both methane and water solids.

■ ASSOCIATED CONTENT

Ⓢ Supporting Information

The Supporting Information is available free of charge at https://pubs.acs.org/doi/10.1021/acs.jpcc.2c05824.

> Crystal quality of the starting samples, pressure shift coefficients of the lattice phonons, and C−H stretching modes of methane clathrate hydrate measured in phases MH-I, MH-II, and MH-III; IR absorption spectra measured in a sapphire anvil cell showing the decomposition of MH-I crystalline samples at two different pressures; and details of the kinetics study of the crystallization of MH-II (PDF)

■ AUTHOR INFORMATION

Corresponding Author

Roberto Bini − *Dipartimento di Chimica "Ugo Schiff", Università di Firenze, I-50019 Sesto Fiorentino, Italy; LENS, European Laboratory for Non-linear Spectroscopy, I-50019 Sesto Fiorentino, Italy; ICCOM-CNR, Istituto di Chimica dei Composti OrganoMetallici, I-50019 Sesto Fiorentino, Italy;* orcid.org/0000-0002-6746-696X; Phone: +390554572489; Email: roberto.bini@unifi.it

Authors

Demetrio Scelta − *ICCOM-CNR, Istituto di Chimica dei Composti OrganoMetallici, I-50019 Sesto Fiorentino, Italy; LENS, European Laboratory for Non-linear Spectroscopy, I-50019 Sesto Fiorentino, Italy;* orcid.org/0000-0002-4856-0125

Samuele Fanetti − *ICCOM-CNR, Istituto di Chimica dei Composti OrganoMetallici, I-50019 Sesto Fiorentino, Italy; LENS, European Laboratory for Non-linear Spectroscopy, I-50019 Sesto Fiorentino, Italy;* orcid.org/0000-0002-5688-6272

Selene Berni − *LENS, European Laboratory for Non-linear Spectroscopy, I-50019 Sesto Fiorentino, Italy;* ⊙ orcid.org/0000-0002-9022-6163

Matteo Ceppatelli − *ICCOM-CNR, Istituto di Chimica dei Composti OrganoMetallici, I-50019 Sesto Fiorentino, Italy; LENS, European Laboratory for Non-linear Spectroscopy, I-50019 Sesto Fiorentino, Italy;* ⊙ orcid.org/0000-0002-0688-5167

Notes
The authors declare no competing financial interest.

■ REFERENCES

(1) Buffett, B. A. Clathrate Hydrates. *Annu. Rev. Earth Planet. Sci.* **2000**, *28*, 477−507.

(2) Collett, T.; Bahk, J.-J.; Baker, R.; Boswell, R.; Divins, D.; Frye, M.; Goldberg, D.; Husebø, J.; Koh, C.; Malone, M.; et al. Methane Hydrates in Nature-Current Knowledge and Challenges. *J. Chem. Eng. Data* **2015**, *60*, 319−329.

(3) Milkov, A. V. Global Estimates of Hydrate-Bound Gas in Marine Sediments: How Much is Really Out There? *Earth-Sci. Rev.* **2004**, *66*, 183−197.

(4) Hassanpouryouzband, A.; Joonaki, E.; Vasheghani Farahani, M. V.; Takeya, S.; Ruppel, C.; Yang, J.; English, N. J.; Schicks, J. M.; Edlmann, K.; Mehrabian, H.; et al. Gas Hydrates in Sustainable Chemistry. *Chem. Soc. Rev.* **2020**, *49*, 5225−5309.

(5) Froitzheim, N.; Majka, J.; Zastrozhnov, D. Methane Release from Carbonate Rock Formations in the Siberian Permafrost Area During and after the 2020 Heat Wave. *Proc. Natl. Acad. Sci. U.S.A.* **2021**, *118*, No. e2107632118.

(6) Ruppel, C. D.; Kessler, J. D. The Interaction of Climate Change and Methane Hydrates. *Rev. Geophys.* **2017**, *55*, 126−168.

(7) Loveday, J. S.; Nelmes, R. J.; Guthrie, M.; Belmonte, S. A.; Allan, D. R.; Klug, D. D.; Tse, J. S.; Handa, Y. P. Stable methane hydrate above 2 GPa and the source of Titan's atmospheric methane. *Nature* **2001**, *410*, 661−663.

(8) Mousis, O.; Gautier, D.; Bockelee-Morvan, D. An Evolutionary Turbulent Model of Saturn's Subnebula: Implications for the Origin of the Atmosphere of Titan. *Icarus* **2002**, *156*, 162−175.

(9) Niemann, H.; Atreya, S.; Bauer, S.; Carignan, G. R.; Demick, J. E.; Frost, R. L.; Gautier, D.; Haberman, J. A.; Harpold, D. N.; Hunten, D. M.; et al. The abundances of constituents of Titan's atmosphere from the GCMS instrument on the Huygens probe. *Nature* **2005**, *438*, 779−784.

(10) Fortes, A. D.; Choukroun, M. Phase Behaviour of Ices and Hydrates. *Space Sci. Rev.* **2010**, *153*, 185−218.

(11) Lunine, J.; Choukroun, M.; Stevenson, D.; Tobie, G. The Origin and Evolution of Titan. In *Titan from Cassini-Huygens*; Brown, R. H., Lebreton, J. P., Waite, J. H., Eds.; Springer: Dordrecht, 2009; pp 33−59.

(12) Hayes, A. G.; Lorenz, R. D.; Lunine, J. I. A post-Cassini view of Titan's methane-based hydrologic cycle. *Nat. Geosci.* **2018**, *11*, 306−313.

(13) Choukroun, M.; Grasset, O.; Tobie, G.; Sotin, C. Stability of methane clathrate hydrates under pressure: Influence on outgassing processes of methane on Titan. *Icarus* **2010**, *205*, 581−593.

(14) Grasset, O.; Pargamin, J. The ammonia-water system at high pressures: Implications for the methane of Titan. *Planet. Space Sci.* **2005**, *53*, 371−384.

(15) Bezacier, L.; Le Menn, E.; Grasset, O.; Bollengier, O.; Oancea, A.; Mezouar, M.; Tobie, G. Experimental investigation of methane hydrates dissociation up to 5GPa: Implications for Titan's interior. *Phys. Earth Planet. In.* **2014**, *229*, 144−152.

(16) Fortes, A. D. Titan's internal structure and the evolutionary consequences. *Planet. Space Sci.* **2012**, *60*, 10−17.

(17) Schaack, S.; Ranieri, U.; Depondt, P.; Gaal, R.; Kuhs, W. F.; Gillet, P.; Finocchi, F.; Bove, L. E. Observation of Methane Filled Hexagonal Ice Stable up to 150 GPa. *Proc. Natl. Acad. Sci. U.S.A.* **2019**, *116*, 16204−16209.

(18) Kurnosov, A.; Dubrovinsky, L.; Kuznetsov, A.; Dmitriev, V. High-pressure / High-temperature Behavior of the Methane-Ammonia- Water System up to 3 GPa. *Z. Naturforsch., B: J. Chem. Sci.* **2006**, *61*, 1573−1576.

(19) Kadobayashi, H.; Hirai, H.; Suzuki, K.; Ohfuji, H.; Muraoka, M.; Yoshida, S.; Yamamoto, Y. Sequential in situ Raman spectroscopy for observing dissociation behavior of filled-ice Ih of methane hydrate at high pressure. *J. Raman Spectrosc.* **2020**, *51*, 2536−2542.

(20) Kadobayashi, H.; Ohfuji, H.; Hirai, H.; Ohtake, M.; Yamamoto, Y. Stability of Methane Hydrate at High-Pressure and High-Temperature of up to 40 GPa and 573 K. *J. Phys.: Conf. Ser.* **2020**, *1609*, 012007.

(21) Pruteanu, C. G.; Ackland, G. J.; Poon, W. C.; Loveday, J. S. When Immiscible Becomes Miscible-Methane in Water at High Pressures. *Sci. Adv.* **2017**, *3*, No. e1700240.

(22) Duan, Z.; Mao, S. A. A thermodynamic model for calculating methane solubility, density and gas phase composition of methane-bearing aqueous fluids from 273 to 523K and from 1 to 2000bar. *Geochim. Cosmochim. Acta* **2006**, *70*, 3369−3386.

(23) Pruteanu, C. G.; Naden Robinson, V. N.; Ansari, N.; Hassanali, A.; Scandolo, S.; Loveday, J. S. Squeezing Oil into Water under Pressure: Inverting the Hydrophobic Effect. *J. Phys. Chem. Lett.* **2020**, *11*, 4826−4833.

(24) Chandler, D. Interfaces and the Driving Force of Hydrophobic Assembly. *Nature* **2005**, *437*, 640−647.

(25) Ceppatelli, M.; Bini, R.; Schettino, V. High-Pressure Photodissociation of Water as a Tool for Hydrogen Synthesis and Fundamental Chemistry. *Proc. Natl. Acad. Sci. U.S.A.* **2009**, *106*, 11454−11459.

(26) Ceppatelli, M.; Bini, R.; Schettino, V. High-Pressure Reactivity of Model Hydrocarbons Driven by Near-UV Photodissociation of Water. *J. Phys. Chem. B* **2009**, *113*, 14640−14647.

(27) Ceppatelli, M.; Bini, R.; Schettino, V. High-pressure Reactivity of Clathrate Hydrates by Two-Photon Dissociation of Water. *Phys. Chem. Chem. Phys.* **2011**, *13*, 1264−1275.

(28) Bini, R.; Schettino, V. *Materials under Extreme Conditions: Molecular Crystals at High Pressure*; Imperial College Press: London, 2013.

(29) MacKenzie, S. M.; Birch, S. P. D.; Hörst, S.; Sotin, C.; Barth, E.; Lora, J. M.; Trainer, M. G.; Corlies, P.; Malaska, M. J.; Sciamma-O'Brien, E.; et al. Titan: Earth-like on the Outside, Ocean World on the Inside. *Planet. Sci. J.* **2021**, *2*, 112.

(30) Mao, H. K.; Bell, P. M.; Shaner, J. V.; Steinberg, D. J. Specific volume measurements of Cu, Mo, Pd, and Ag and calibration of the rubyR1fluorescence pressure gauge from 0.06 to 1 Mbar. *J. Appl. Phys.* **1978**, *49*, 3276−3283.

(31) Bini, R.; Ballerini, R.; Pratesi, G.; Jodl, H. J. Experimental Setup for Fourier Transform Infrared Spectroscopy Studies in Condensed Matter at High Pressure and Low Temperatures. *Rev. Sci. Instrum.* **1997**, *68*, 3154−3160.

(32) Ceppatelli, M.; Gorelli, F. A.; Haines, J.; Santoro, M.; Bini, R. Probing High-Pressure Reactions in Heterogeneous Materials by Raman Spectroscopy. *Z. Kristallogr.* **2014**, *229*, 83−91.

(33) Shimizu, H.; Kumazaki, T.; Kume, T.; Sasaki, S. In Situ Observations of High-Pressure Phase Transformations in a Synthetic Methane Hydrate. *J. Phys. Chem. B* **2002**, *106*, 30−33.

(34) Kumazaki, T.; Kito, Y.; Sasaki, S.; Kume, T.; Shimizu, H. Single-Crystal Growth of the High-Pressure Phase II of Methane Hydrate and its Raman Scattering Study. *Chem. Phys. Lett.* **2004**, *388*, 18−22.

(35) Sasaki, S.; Kito, Y.; Kume, T.; Shimizu, H. High-Pressure Raman Study on the Guest Vibration in the Host Cage of Methane Hydrate Structure I. *Chem. Phys. Lett.* **2007**, *444*, 91−95.

(36) Choukroun, M.; Morizet, Y.; Grasset, O. Raman Study of Methane Clathrate Hydrates under Pressure: New Evidence for the Metastability of Structure II. *J. Raman Spectrosc.* **2007**, *38*, 440−451.

(37) Hirai, H.; Uchihara, Y.; Fujihisa, H.; Sakashita, M.; Katoh, E.; Aoki, K.; Nagashima, K.; Yamamoto, Y.; Yagi, T. High-Pressure Structures of Methane Hydrate Observed up to 8 GPa at Room Temperature. *J. Chem. Phys.* **2001**, *115*, 7066−7070.

(38) Ohtani, T.; Ohno, Y.; Sasaki, S.; Kume, T.; Shimizu, H. High-pressure Raman study of methane hydrate "filled ice". *J. Phys.: Conf. Ser.* **2010**, *215*, 012058.

(39) Chen, J.-Y.; Yoo, C.-S. Formation and Phase Transitions of Methane Hydrates under Dynamic Loadings: Compression Rate Dependent Kinetics. *J. Chem. Phys.* **2012**, *136*, 114513.

(40) Minceva-Sukarova, B.; Sherman, W. F.; Wilkinson, G. R. The Raman spectra of ice (Ih, II, III, V, VI and IX) as functions of pressure and temperature. *J. Phys. C: Solid State Phys.* **1984**, *17*, 5833−5850.

(41) Loveday, J. S.; Nelmes, R. J.; Guthrie, M.; Klug, D. D.; Tse, J. S. Transition from Cage Clathrate to Filled Ice: the Structure of Methane Hydrate III. *J. Phys. Rev. Lett.* **2001**, *87*, 215501.

(42) Celli, M.; Ulivi, L.; del Rosso, L. Raman Investigation of the Ice Ic-Ice Ih Transformation. *J. Phys. Chem. C* **2020**, *124*, 17135−17140.

(43) Fanetti, S.; Scelta, D.; Bini, R. Growth Dynamics of Crystalline Ar Hydrate. *J. Phys. Chem. C* **2020**, *124*, 10159−10166.

(44) Fanetti, S.; Falsini, N.; Bartolini, P.; Citroni, M.; Lapini, A.; Taschin, A.; Bini, R. Superheating and Homogeneous Melting Dynamics of Bulk Ice. *J. Phys. Chem. Lett.* **2019**, *10*, 4517−4522.

(45) Verma, P. K.; Kundu, A.; Puretz, M. S.; Dhoonmoon, C.; Chegwidden, O. S.; Londergan, C. H.; Cho, M. The Bend+Libration Combination Band Is an Intrinsic, Collective, and Strongly Solute-Dependent Reporter on the Hydrogen Bonding Network of Liquid Water. *J. Phys. Chem. B* **2018**, *122*, 2587−2599.

(46) Dyadin, Y. A.; Aladko, E. Ya.; Larionov, E. G. Decomposition of Methane Hydrates up to 15 kbar. *Mendeleev Commun.* **1997**, *7*, 34−35.

(47) Umemoto, S.; Yoshii, T.; Akahama, Y.; Kawamura, H. X-ray Diffraction Measurements for Solid Methane at High Pressures. *J. Phys.: Condens. Matter* **2002**, *14*, 10675.

(48) Bezacier, L.; Journaux, B.; Perrillat, J.-P.; Cardon, H.; Hanfland, M.; Daniel, I. Equations of State of Ice VI and Ice VII at High Pressure and High Temperature. *J. Chem. Phys.* **2014**, *141*, 104505.

(49) Hummer, G.; Garde, S.; García, A. E.; Paulaitis, M. E.; Pratt, L. R. The Pressure Dependence of Hydrophobic Interactions is Consistent with the Observed Pressure Denaturation of Proteins. *Proc. Natl. Acad. Sci. U.S.A.* **1998**, *95*, 1552−1555.

(50) Hazen, R. M.; Mao, H. K.; Finger, L. W.; Bell, P. M. Structure and Compression of Crystalline Methane at High Pressure and Room Temperature. *App. Phys. Lett.* **1980**, *37*, 288−289.

(51) Abramson, E. H. Melting Curves of Argon and Methane. *High Pressure Res.* **2011**, *31*, 549−554.

(52) Yagi, T.; Suzuki, H. Melting curve of methane to 4.8GPa determined by the ruby pressure-temperature marker. *Proc. Jpn. Acad., Ser. B* **1990**, *66*, 167−172.

(53) Soper, A. K. Water and Ice. *Science* **2002**, *297*, 1288−1289.

(54) Datchi, F.; Loubeyre, P.; LeToullec, R. Extended and accurate determination of the melting curves of argon, helium, ice(H2O),and hydrogen(H2). *Phys. Rev. B: Condens. Matter Mater. Phys.* **2000**, *61*, 6535−6546.